MODELLING, DESIGN, AND PERFORMANCE EVALUATION OF AN LCL FILTER FOR THREE-PHASE POWER CONVERTERS CONNECTED TO THE GRID

Abstract

The utilization of Power Converters for the purpose of integrating renewable power sources with the alternating current (AC) grid has experienced a notable rise over the past twenty years. An LCL filter is commonly employed for the purpose of connecting Power Converters to the utility grid, with the intention of mitigating the presence of high order harmonics generated by the Converter. In order to attain the desired level of filtering performance that adheres to the strict grid code requirement while also considering cost and effectiveness, it is necessary to implement an optimized design for the LCL filter. This document introduces a study on the modelling and design methodology of an LCL filter for grid-interconnected converters, employing an analytical approach. The simulation results demonstrate that by employing this design methodology, there is a reduction of 98.51% in the current harmonics observed at the output of the converter. The LCL filter is a component used in power converters to reduce the Total Harmonic Distortion (THD) of the output waveform. It achieves this by providing passive damping.

Keywords: LCL Filter, Power Converter, Total Harmonic Distortion (THD), Passive Damping

Authors

Dipak Kumar Dash
Department of Electrical Engineering
IIT(ISM)
Dhanbad, India.

Alok Kumar Shrivastav
Department of Electrical Engineering
JIS College of Engineering
Kalyani, India
alok5497@gmail.com

Moumita Pal
Department of Electronics & Communication Engineering
JIS College of Engineering
Kalyani, India

Partha Sarkar
Department of Electronics & Communication Engineering
JIS College of Engineering
Kalyani, India

I. OVERVIEW

The utilisation of Power Converters for grid interconnection has been experiencing growth in various applications, including power quality, regenerative motor drive, and distributed generation (DG) (John et al., 2009). Different types of distributed generation systems, such as photo-voltaic (PV) and fuel cells, generate electrical energy in the form of direct current (DC) voltage sources. Additionally, wind energy generation typically involves the production of alternating current (AC), which is often subsequently converted to direct current (DC). Therefore, when connected to a direct current to alternating current inverter, these distributed generation systems have the capability to provide electrical energy to the utility grid. Nevertheless, the power electronic devices employed in voltage source inverters (VSI) introduce unwanted harmonics that impact the adjacent loads at the point of common coupling (PCC) with the utility grid, thereby violating the standard norms for grid interconnection.

Therefore, in order to connect these voltage source inverters (VSI) to the utility grid, it is often necessary to incorporate a filter that can effectively mitigate the presence of harmonics in the output current, ensuring that they are within acceptable limits (Sarkar, 2015). The LCL-filter is considered to be one of the most efficient filters for voltage source inverters (VSI) that are connected to the grid (Jayalath and Hanif, 2017b). The design of filters utilized in grid-connected inverter applications encompasses a multitude of constraints. The filter requirements are determined by the precise tolerances set by standards such as IEEE 519-1992, which provides recommended practices and requirements for controlling harmonics in electrical power systems. Other standards, such as IEEE 1547.2-2008, offer guidance on applying the IEEE standard for interconnecting distributed resources with electric power systems. These standards, along with considerations for reactive power compensation limits and the maximum allowable voltage drop across the filter, help to restrict switching losses. (John et al., 2009; IEEE Standard 519 – 1992 1993; IEEE Standard 1547.1 – 2005 2005; Jayalath and Hanif, 2017b). The utilization of higher order LCL filters is necessary in order to meet the regulatory standards in a compact and lightweight manner (John et al., 2009). The iterative process is necessary for designing the parameters of the LCL filter, including the inductors and capacitors on both the grid-side and inverter-side. This is because there is a correlation between the filter parameters and the specific design requirements, as discussed by Jayalath and Hanif in their 2017a study. The primary aim of this paper is to present design methodologies for higher order LCL filters and offer guidance on achieving optimized filter design.

Superiority of a High-Order Filter compared to a First-Order Filter: The first-order L filter, although straightforward, is characterised by its large size and inability to meet the rigorous requirements for harmonic attenuation as outlined in the study by Channegowda et al. (2010). The utilisation of a third order LCL filter has become prevalent in order to achieve increased attenuation, as demonstrated by Karshenas and Saghafi in 2006. This approach also allows for significant reductions in the size and cost of the components, as highlighted by Liserre et al. in 2005 and Channegowda et al. in 2010. However, the systematic design of an LCL filter is a challenging task (Jayalath and Hanif, 2017a). Several crucial factors, such as output current ripple, current harmonics generated by insulated gate bipolar transistor (IGBT) switches, series fundamental drop, desired power factor, resonance frequency, and control stability, must be carefully taken into account (Liserre et al., 2005; Channegowda et al.,

2010). Furthermore, it is imperative to consider the aggregate dimensions and financial implications of the constituent elements when choosing different parameters for an optimal design. Figure 1 provides a comparative analysis of a first-order (L) filter and a third-order (LCL) filter. The data demonstrates that a third-order filter exhibits enhanced performance in suppressing higher harmonic frequencies. Consequently, it can be specifically engineered to fulfil the rigorous requirements for harmonic attenuation. This phenomenon occurs due to the fact that, for an equivalent or lower net inductance (L1+L2), a third-order filter exhibits superior attenuation (60dB/decade) at frequencies beyond the resonance frequency.

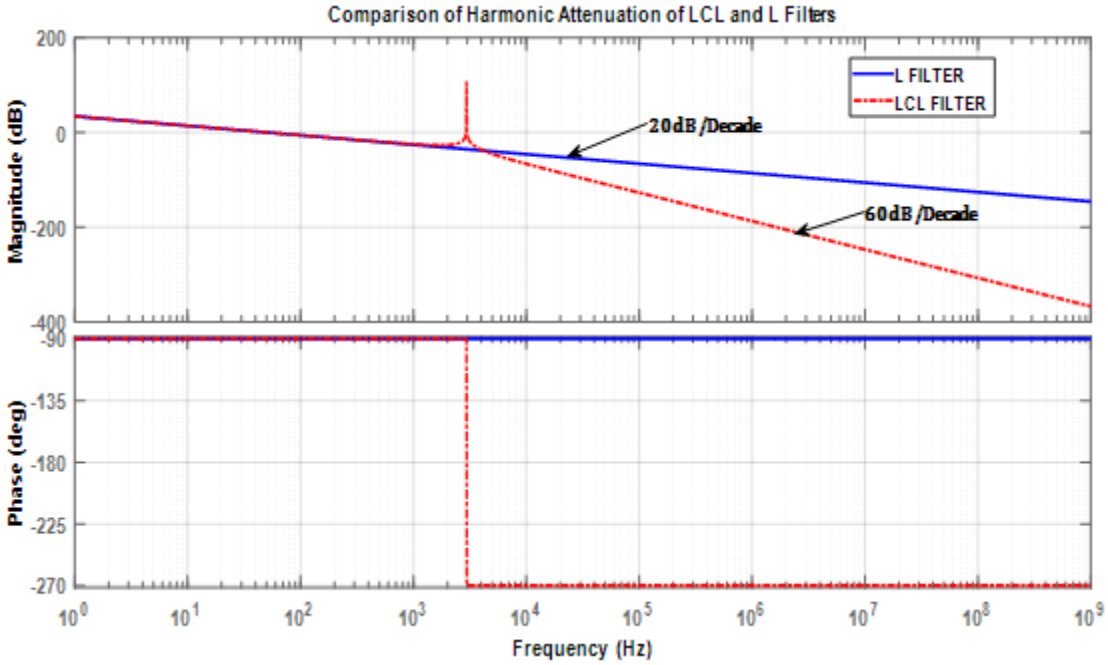

Figure 1: Comparative Analysis of Harmonic Attenuation between LCL and L Filters

II. ANALYSIS OF HARMONIC CHARACTERISTICS IN PHOTOVOLTAIC INVERTER SYSTEM

The determination of the level and sequence of harmonics in the output of a Voltage Source Inverter (VSI) is performed. Characterization is performed in order to determine the extent of harmonics present in the output of a Voltage Source Inverter (VSI).

In this scenario, the Voltage Source Inverter (VSI) was integrated into a Simulink interface, allowing for the examination of the VSI's output in relation to the harmonic composition and distortion present in the current waveform. Figure 2 depicts the Simulink model utilised for the characterization process.

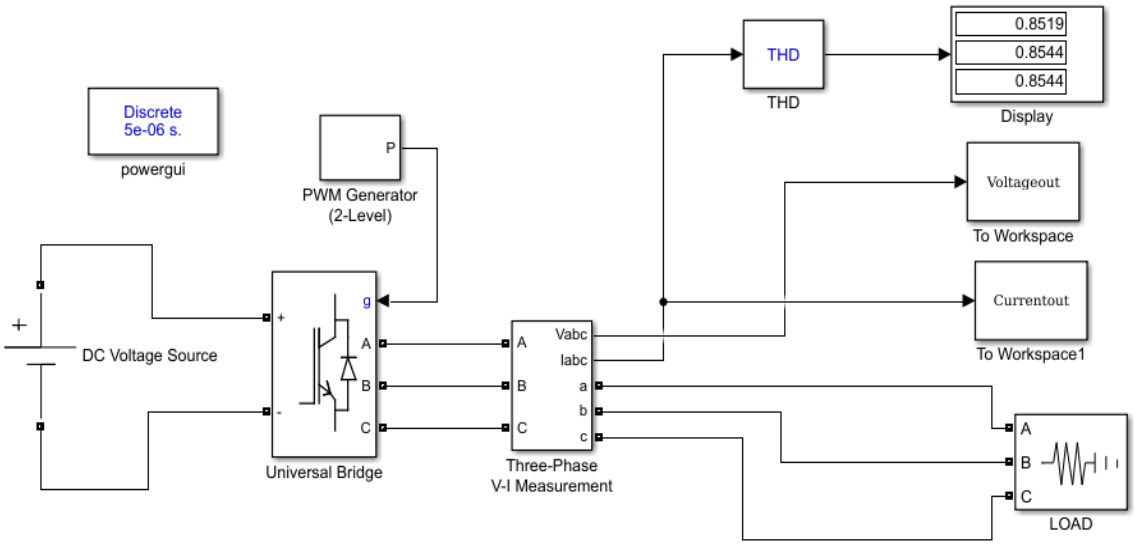

Figure 2

Figure 2 Display the Simulink model utilized for the purpose of characterizing Harmonics in a Photovoltaic (PV) Inverter System

1. **Modelling and Design of LCL Filter:** This section focuses on the process of creating a mathematical model and designing an LCL filter. The transfer function model of the LCL filter is derived and the model parameters are obtained using a well-defined design procedure. The process of modelling and designing the LCL filter involves determining the specific parameter values for the filter. The LCL filter is employed to alleviate higher order harmonics that are present at the output of the Voltage Source Inverter (VSI). A mathematical model is formulated utilising the power circuit of a three-phase grid-connected Voltage Source Inverter (VSI) with an LCL (Inductor-Capacitor-Inductor) filter. The three-phase power circuit is converted into a simplified single-phase equivalent circuit. The transfer function of the LCL filter is then determined using the parameters of the circuit.

   Mathematical model for the LCL Filter: Figure 3 illustrates the power circuit configuration of a three-phase grid-connected power converter. As illustrated in the diagram and in the Single Phase equivalent circuit shown in Figure 4, the LCL filter serves as an intermediary component between the grid and the power converter. Vg represents the voltage across the grid. L1 and L2 are the inductors on the converter side and grid side, respectively, of the LCL filter. The term "C" is an abbreviation for the LCL filter capacitor, which is used in the context of electrical circuits. Similarly, "RD" stands for the damping resistor, which serves a specific purpose in the circuit. VDC refers to the direct current (DC) bus voltage.

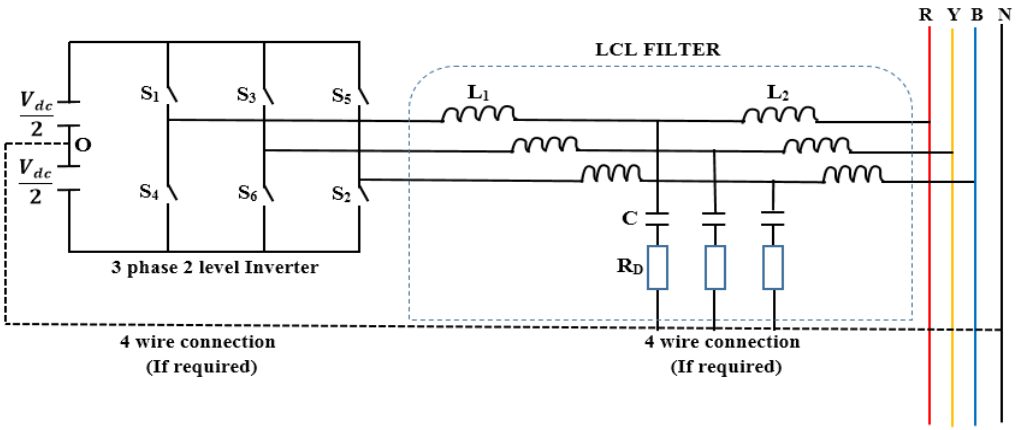

Figure 3

Figure 3 illustrates the power circuit diagram of a three-phase grid-connected inverter equipped with an LCL filter.

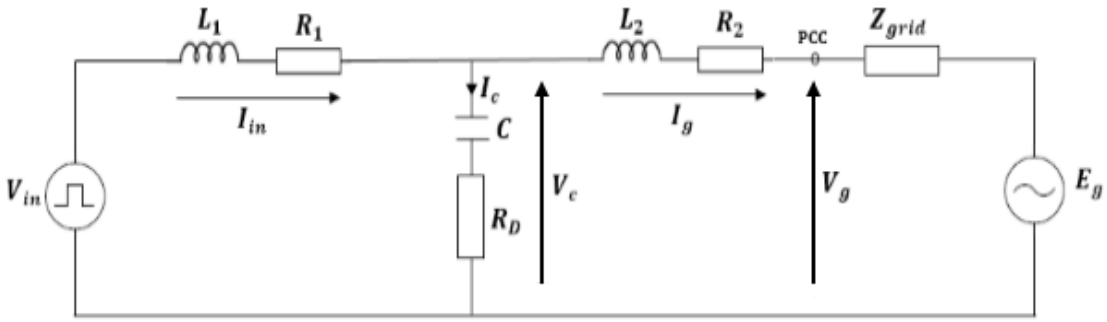

Figure 4

Figure 4 illustrates the single-phase equivalent circuit.

In the LCL filter model, it is assumed that;

At frequencies that are not the fundamental frequency, the grid exhibits characteristics similar to a short circuit. The value of the variable "Vg" is equal to zero.

The transfer function for the LCL filter is a crucial component.

$$H = \frac{i_g}{V_{in}} = \frac{Filter\ output\ current}{input\ voltage} \tag{2.1}$$

Hence, H can be defined as the transfer function of admittance. In the complex S domain, the following equation holds true:

$$H(s) = \frac{I_g(s)}{V_{in}(s)} \tag{2.2}$$

By utilising Kirchhoff's laws, the circuit depicted in Figure 4 can be represented as an equivalent circuit. The mathematical representation of the filter in the s-plane can be expressed through the following equations:

$$I_{in} - I_c - I_g = 0 \quad (2.3)$$
$$V_{in} - V_c = I_{in}(sL_1 + R_1) \quad (2.4)$$
$$V_c - V_g = I_g(sL_2 + R_2) \quad (2.5)$$
$$V_c = I_c\left(\frac{1}{sC} + R_D\right) \quad (2.6)$$

The circuit parameters are formally specified as;

V_{in}	Inverter Voltage
I_{in}	Inverter Current
V_c	Voltage across Filter Capacitor
I_c	Filter Capacitor Current
I_g	Grid Current
L_1	Inverter side inductor
L_2	Grid side inductor
C	Capacitor
R_D	Damping Resistor
V_g	Grid voltage
R_1	Inverter Side Parasitic Resistance
R_2	Grid Side Parasitic Resistance

The grid side parasitic resistance refers to the resistance that is present in the electrical grid system. It is a measure of the opposition to the flow of electric current in the grid, caused by various factors such as

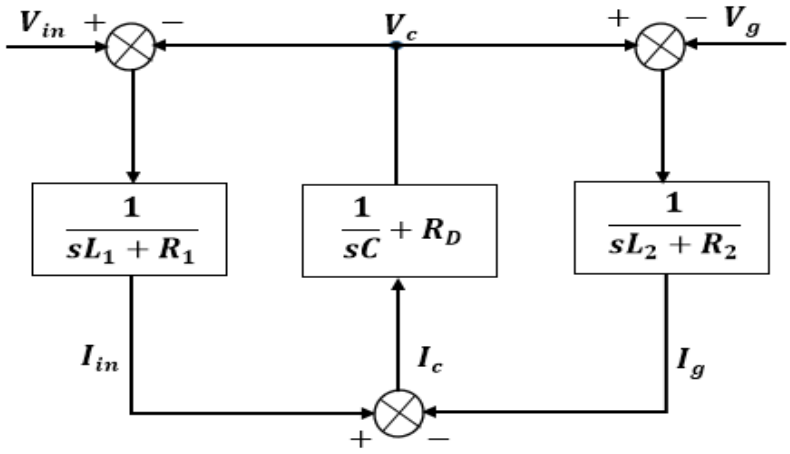

Figure 5

Figure 5 depicts the block diagram of the LCL Filter in the frequency domain.

It is important to note that when considering frequencies other than the fundamental frequency, the voltage gain (Vg) is equal to zero.

Substituting Vg = 0 into equation 2.5 yields:

$$V_c = I_g(sL_2 + R_2) \tag{2.7}$$

Performing the mathematical operation of equating the numerical values 2.6 and 2.7 results in;

$$I_g(sL_2 + R_2) = I_c\left(\frac{1}{sC} + R_D\right) \tag{2.8}$$

The value of 0 in equation 3.5 corresponds to the mental component in the frequency domain.

$$I_c = I_g\left(\frac{s^2CL_2 + sCR_2}{sCR_D + 1}\right) \tag{2.9}$$

Based on the mathematical expression denoted as equation 2.3,

$$I_{in} = I_c + I_g \tag{2.10}$$

Substituting equation 2.9 into equation 2.10 yields:

$$I_{in} = I_g + I_g\left(\frac{s^2CL_2 + sCR_2}{sCR_D + 1}\right) \tag{2.11}$$

Additionally, based on equation 2.4,

$$V_{in} = V_c + I_{in}(sL_1 + R_1) \tag{2.12}$$

By substituting equations 2.7 and 2.11 into equation 2.12, we obtain:

$$V_{in} = I_g(sL_2 + R_2) + (sL_1 + R_1)\left[I_g + I_g\left(\frac{s^2CL_2 + sCR_2}{sCR_D + 1}\right)\right] \tag{2.13}$$

$$V_{in} = I_g\left[(sL_1 + R_1) + (sL_2 + R_2) + \frac{(sL_1 + R_1)(s^2CL_2 + sCR_2)}{sCR_D + 1}\right] \tag{2.14}$$

$$V_{in} = I_g\left[\frac{\begin{matrix}s^3CL_1L_2 + s^2C(L_1(R_2 + R_D) + L_2(R_1 + R_D)) + \\ s\big(L_1 + L_2 + C(R_1R_2 + R_1R_D + R_2R_D)\big) + R_1 + R_2\end{matrix}}{sCR_D + 1}\right] \tag{2.15}$$

Hence, the transfer function as per equation 2.2 can be expressed as:

$$Hd_{LCL}(s) = \frac{sCR_D + 1}{\begin{matrix}s^3CL_1L_2 + s^2C(L_1(R_2 + R_D) + L_2(R_1 + R_D)) + \\ s\big(L_1 + L_2 + C(R_1R_2 + R_1R_D + R_2R_D)\big) + R_1 + R_2\end{matrix}} \tag{2.16}$$

In the absence of the damping resistance RD, equation 2.16 is modified as follows:

$$H_{LCL}(s) = \frac{1}{s^3 C L_1 L_2 + s^2 C(L_1 R_2 + L_2 R_1) + s\left(L_1 + L_2 + C(R_1 R_2)\right) + R_1 + R_2} \quad (2.17)$$

Figure 6 depicts the Bode plots of the LCL filter, both with and without damping. By introducing a resistor in series with the capacitor, the amplification spike is mitigated, resulting in a more even response and a roll-off of -180 degrees at high frequencies, as opposed to -270 degrees. The LCL filter exhibits excellent high-frequency performance, demonstrating an attenuation rate of -60 dB per decade.

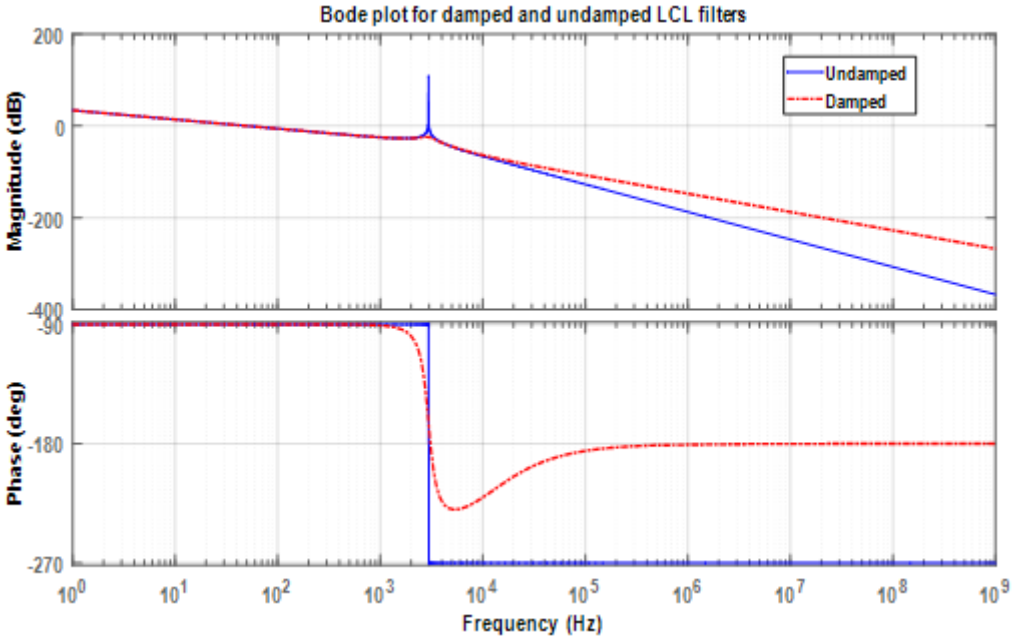

Figure 6

Figure 6 displays the Bode plot illustrating the frequency response characteristics of both damped and undamped LCL filters.

2. **Low-Current Limit (LCL) Filter Design Procedure:** The LCL filter design methodology is focused on meeting grid code requirements by effectively reducing the amplitude of high order current harmonic components on the grid side. The nominal system parameters that are required are as follows. Table 1 presents the nominal system parameters employed in the design process.

Fundamental values:

Base voltage $= V_B = E_n = \sqrt{3} \times V_g = \sqrt{3} \times 240 = 415V$

Base Impedance $= Z_B = \frac{{E_n}^2}{P_n} = \frac{415^2}{100000} = 1.7223\Omega$

Base angular frequency $= \omega_g = 2\pi f_g = 2\pi \times 50 = 314.2\ rads$

$$\text{Base Capacitance} = \mathrm{C}_B = \frac{1}{\omega_g \mathrm{Z}_B} = \frac{1}{314.2 \times 1.7223} = 1847.93\mu F$$

$$\text{Base Inductance} = \mathrm{L}_B = \frac{\mathrm{Z}_B}{\omega_g} = \frac{1.7223}{314.2} = 5.482mH$$

The expression of any quantity divided by its base value is denoted in per unit (p.u.) notation. In terms of a standardised unit of measurement.

Key Performance Indicators:

The split factor refers to the ratio between the inductances of the LCL filter.

$$\mathrm{r}_l = \frac{\mathrm{L}_2}{\mathrm{L}_1} \tag{2.18}$$

The ratio between the low-pass filter capacitance (LCL) and the total inductance, expressed in per unit (p.u.), is being requested.

$$\mathrm{r}_q = \frac{c}{\mathrm{l}_T} = \frac{{\mathrm{Z}_B}^2 C}{\mathrm{L}_T} \tag{2.19}$$

The ratio between the switching **frequency** and resonance frequency

$$\mathrm{r}_f = \frac{\mathrm{f}_{sw}}{\mathrm{f}_{res}} = \frac{\omega_{sw}}{\omega_{res}} \tag{2.20}$$

- **Design Criteria for LCL Filters:** The subsequent factors are crucial design criteria for the LCL filter.
  - Achievement of reactive volt-ampere (VAR) limits with power factor approaching unity.
  - The objective is to determine the optimal volume and weight that will result in the minimum cost of passive components, specifically inductive and capacitive components.
  - The output current is designed to have a total harmonic distortion (THD) of less than or equal to 0.03, resulting in the reduction of higher order harmonics.
  - The selection of an appropriate resonance frequency is crucial in order to effectively reduce the switching harmonics and prevent the filter components from becoming excessively large (Sarkar, 2015; Karshenas and Saghafi, 2006; Ben Said-Romdhane et al., 2017).

- **Design of Inductance on the Inverter Side:** In the initial stage, it is necessary to undertake the design of the inductance on the inverter side. In order to accomplish this task, we have chosen to adopt the approach proposed by Reznik et al. (2013).

  In this context, we are examining the maximum current ripple that exists at the output of an inverter, as denoted by the following equation:

$$\Delta I_{Lmax} = \frac{2V_{DC}}{3L_1}(1-m)mT_{sw} \tag{2.21}$$

Where m represents the modulation index and $T_{sw} = \frac{1}{f_{sw}}$

However, the maximum peak-to-peak current ripple is observed when the modulation index (m) is equal to 0.5. Therefore, equation 2.21 is transformed into:

$$\Delta I_{Lmax} = \frac{V_{DC}}{6 f_{sw} L_1} \quad (2.22)$$

Given the design parameters, equation 2.21 can be expressed to account for a 10% ripple of the rated current.

$$\Delta I_{Lmax} = 0.1 I_{max} \quad (2.23)$$

where.

$$I_{max} = \frac{\sqrt{2} P_n}{3 V_{ph}} \quad (2.24)$$

$$L_1 = \frac{V_{DC}}{6 f_{sw} \Delta I_{Lmax}} \quad (2.25)$$

Based on equation 2.25, it can be inferred that;

$$L_1 = \frac{800}{6 \times 16000 \times 19.642} = 0.424 mH$$

- **Determination of the Maximum Value of the LCL Filter Capacitor:** Decreasing the value of the filter capacitor C will mitigate the passage of excessive reactive currents, thereby minimising unnecessary current flow. It is well-established that the transmission of reactive power is intricately linked to the maintenance of voltage stability. Hence, an increased value of capacitance (C) can potentially lead to voltage instability issues within the electrical grid. In this scenario, the LCL filter capacitor C is configured to ensure that its reactive power consumption is below n% of the rated power Pn, as depicted in Equation (3.26a) (Ben Said-Romdhane et al., 2017). In the given equation, Qc represents the reactive power absorbed by the filter capacitor. The variable n is a positive factor that is typically selected to be equal to or less than 5% (Sarkar, 2015; Ben Said-Romdhane et al., 2017). As per Equations (2.26a) and (2.26b), the upper limit of the filter capacitor can be mathematically represented by Equation (2.26c).

$$Q_C = n\%. P_n \quad 2.26a$$

However,

$$Q_C = -{E_n}^2 C \omega_g \quad 2.26b$$

This suggests that when n is equal to 5%,

$$\mathrm{C}_{max} = 0.05 \left(\frac{P_n}{3 {V_g}^2 \omega_g} \right) \quad 2.26c$$

$$\mathrm{C}_{max} = 92.4 \mu F$$

In this scenario, the value of C is equal to the maximum capacitance Cmax, which precisely amounts to 5% of the base capacitance CB.

- **Design of Grid-Side Inductance:** In order to achieve a 20% reduction in ripple on the grid side compared to the current ripple on the inverter side, certain measures need to be implemented.

$$L_2 = \frac{\sqrt{\frac{1}{k^2}} + 1}{C{f_{sw}}^2} \quad (2.27)$$

The attenuation factor, denoted as k in equation 2.27, is assigned a numerical value of 0.2, which corresponds to a 20% reduction.

$$L_2 = \frac{\sqrt{\frac{1}{0.2^2}} + 1}{92.4 \times 10^{-6} \times 16000^2} = 0.254mH$$

- **Designing for Resonance Frequency:** The resonance frequency is contingent upon the values of the filter inductors L1 and L2, as well as the filter capacitor C.

Let us proceed with the technical aspects:

$$\mathrm{L} = \mathrm{L}_1 + \mathrm{L}_2 \; and \; \mathrm{L}_p = \frac{\mathrm{L}_1\mathrm{L}_2}{\mathrm{L}_1 + \mathrm{L}_2}$$

In the context of tank circuits, it can be generally stated that

$$\omega_{res} = \frac{1}{\sqrt{LC}}$$

Therefore, in the context of the LCL filter,

$$\omega_{res} = \frac{1}{\sqrt{L_p C}} \quad 2.28$$

Additionally, the computed value of "x" must adhere to the inequality stated in equation 2.29. Alternatively, the values of equation 3.27 are selected again.

$$10f_g \leq f_{res} \leq 0.5f_{sw} \quad (2.29)$$

Please be aware that the value is expressed in radians.

$$\omega_{res} = \frac{1}{\sqrt{0.000158843 \times 92.4 \times 10^{-6}}} = 8254.29 \; rads/sec$$

$$\mathrm{f}_{res} = \frac{8254.29}{2\pi} = 1313.71Hz$$

Based on equation 2.28;

In this scenario, f_{res} the value of 1500Hz is considered as the frequency (i.e., $\mathrm{fw}_{res} = 9425$ rads/sec) and it meets the condition stated in inequality 2.29.

The minimum DC bus voltage refers to the lowest voltage level that can be sustained in the direct current (DC) bus of a system. As per the findings of Ben Said-Romdhane et al. (2017), the maximum AC voltage that can be generated by a Voltage Source Converter is determined by the DC-bus voltage. A fundamental principle to follow is that the minimum direct current (DC) voltage should be equivalent to the maximum voltage between two phases (line-to-line voltage) of the electrical grid. In the context of a three-phase grid, the mentioned value refers to the maximum magnitude of the voltage measured between any two phases.

Therefore,

$$V_{DCmin} = \sqrt{2}.V_L \quad (2.30)$$

V_L is the line-to-line voltage of the grid.

$V_{DCmin} = 587V$

In this design, V_{DC} is 800V.

The line-to-line voltage refers to the voltage between two phases in an electrical grid. In this particular design, the voltage of the VDC (Voltage Direct Current) is specified as 800 volts.

- **Design of Damping Resistor:** In this design, we incorporate a basic passive damping technique by introducing a resistor RD in series with the capacitor. This configuration helps reduce the amplitude of the ripple occurring at the switching frequency, thus preventing resonance. Based on the findings of Reznik et al. (2013), it is recommended that the resistance value of this particular resistor should be equal to one-third of the impedance of the filter capacitor at the resonance frequency. In other words;

$$R_D = \frac{1}{3\omega_{res} C} \quad (2.31)$$

$$R_D = \frac{1}{3 \times 238.73 \times 92.4 \times 10^{-6}} = 15\Omega$$

Pena-Alzola et al. (2013) provides a mathematical expression for the minimum value of the damping resistor, RDmin. The authors have disclosed that in order to maintain system stability and achieve a positive gain margin in system control, it is necessary for the damping resistor value to adhere to equation 2.32.

$$R_{Dmin} = \frac{1}{3} f_{sw} \left(\frac{{L_2}^2}{L_1 + L_2} \right) \quad (2.32)$$

$$R_{Dmin} = \frac{1}{3} \times 16000 \times 0.000095156 = 0.51\Omega$$

This implies that the selection of RD should be made in a manner that fulfils the given relationship.

$$0.51 \leq R_D \leq 15$$

Note: R_p1 and R_p2 are parasitic resistances associated with the inductors L1 and L2, respectively. These values can be selected directly from the manufacturer's datasheet. In this scenario, the user is referring to a specific situation involving certain variables and conditions.

Table 1 presents the design system parameters that will be employed for the simulation.

- **Simulink model of the Inverter System with the LCL Filter:** Figure 7 depicts the Simulink model representing the Inverter system integrated with the LCL filter. The Simulink model was developed using the design parameters outlined in Table 1 to conduct performance analysis on the LCL filter.

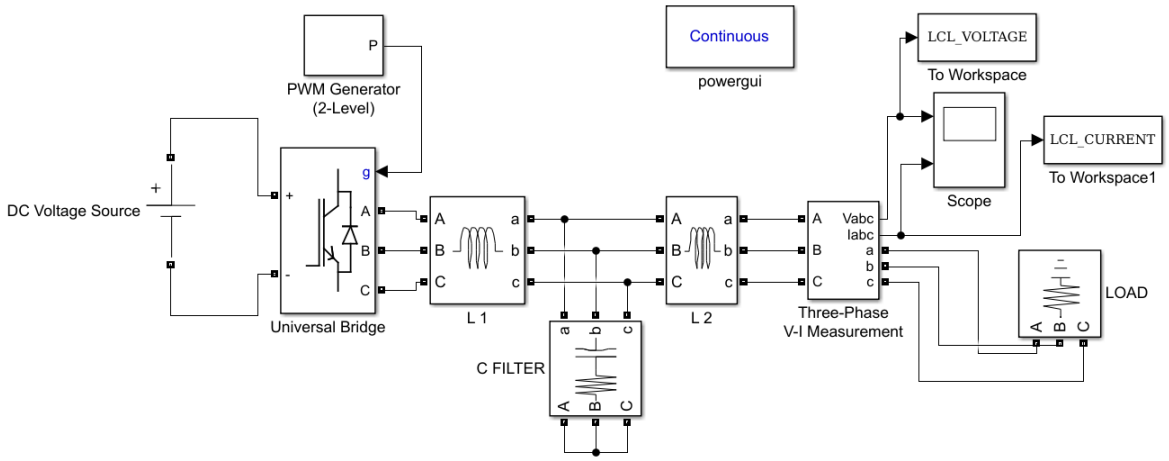

Figure 7

Figure 7 displays the Simulink model representing the Inverter System integrated with the LCL Filter.

III. FINDINGS AND ANALYSIS

1. **Analysis of Harmonics in the Photovoltaic (PV) Inverter System:** This section provides an analysis of the harmonic content found in the unfiltered PV inverter system. The analysis includes the examination of the present waveform and the utilisation of the Fast Fourier Transform (FFT) technique. Based on the analysis of Figure 8 (a), it is evident that the current waveform exhibits a significant deviation from sinusoidal behaviour, primarily attributed to the presence of a substantial amount of harmonics. In Figure 8 (b), the Fast Fourier Transform (FFT) analysis of this system reveals a Total Harmonic Distortion (THD) value of 85.17%. This high THD percentage renders the system impractical and unsuitable for grid-connected applications. Utility operators require that all grid connected systems have a Total Harmonic Distortion (THD) of less than 5%.

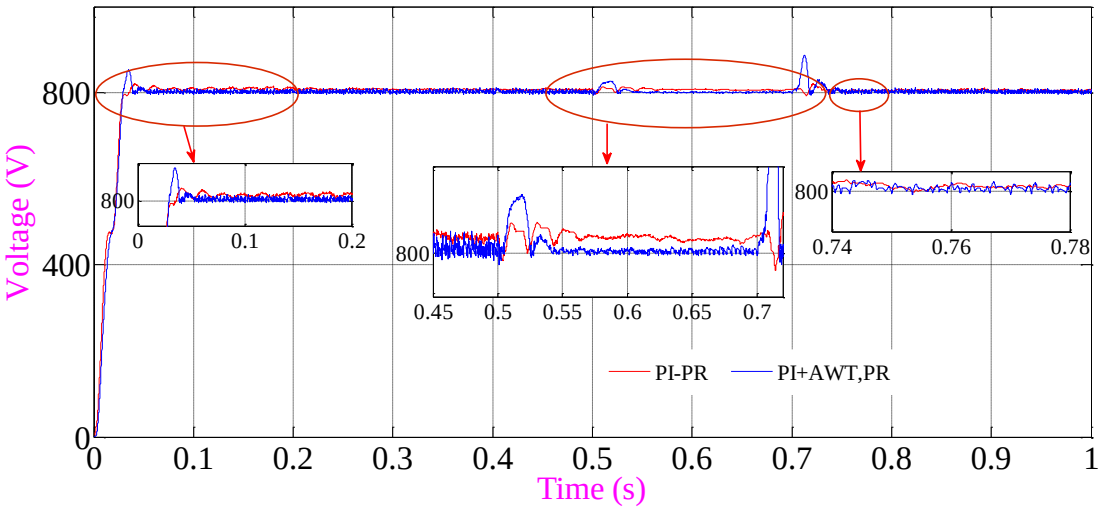

(a)

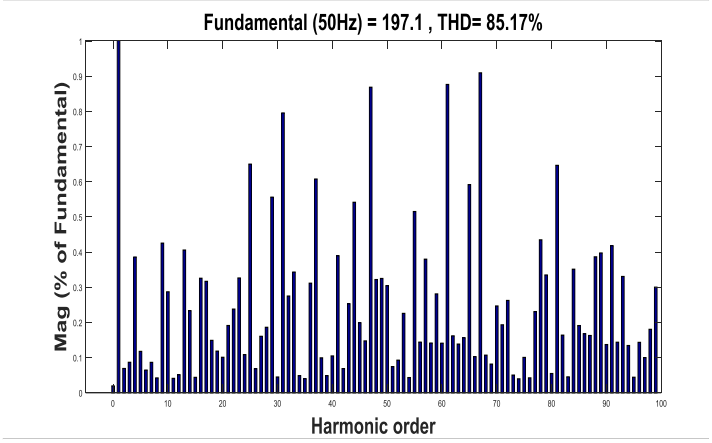

(b)

Figure 8: (a) The graphical representation of the electrical voltage flowing through the PV Inverter System. (b) The application of Fast Fourier Transform (FFT) algorithm to analyse the frequency components present in the PV Inverter System.

Figure 8 showcases the current waveform and Fast Fourier Transform (FFT) analysis of the Photovoltaic (PV) Inverter System.

2. **The Parameters for Simulating the PV Inverter System:** The simulation of the inverter system is conducted using the design parameters acquired in section 2. Table 1 presents the nominal system parameters and design parameters.

Table 1: Design System Parameters

f_g	Grid frequency or fundamental frequency	50Hz
f_{sw}	PWM carrier frequency	16KHz
W_{res}	Resonance frequency	9425 rads/sec

P_n	Rated active power	100KW
E_n	Line to line RMS voltage	$\sqrt{3} \times 240V$
V_{DC}	DC Bus voltage	800V
L_1	Inverter side inductor	0.424mH
L_2	Grid side inductor	0.254mH
R_1	Inverter Side Parasitic Resistance	0.380 Ω
R_2	Grid Side Parasitic Resistance	0.162 Ω
C	Capacitor	92.4μF
R_D	Damping Resistor	2.2Ω
V_g	Grid voltage	240V

The user input "fg" is a command commonly used in Unix-like operating systems to resume

Grid frequency, also known as fundamental frequency, refers to the standard frequency at which an electrical power grid operates. It is the primary frequency at which alternating current (AC) is generated and distributed throughout the grid.

3. **Simulation Results of the LCL Filter:** Figure 9 (a) depicts the waveform of the output current in the inverter system equipped with the LCL filter. At this juncture, it is observed that the waveforms exhibit sinusoidal characteristics due to the effective filtration of a significant proportion of harmonics in the output of the photovoltaic (PV) inverter system by the meticulously engineered LCL filter. The level of harmonic content has been decreased from 85.17% to 1.27%. However, according to Figure 9 (b), it is evident that the LCL filter is not capable of efficiently managing the low order harmonics. Therefore, a current controller is required. The existing controller must incorporate a filtering mechanism to eliminate low order harmonics in order to ensure that the photovoltaic (PV) inverter system complies with the utility's "Standard for Interconnecting Distributed Resources with Electric Power Systems."

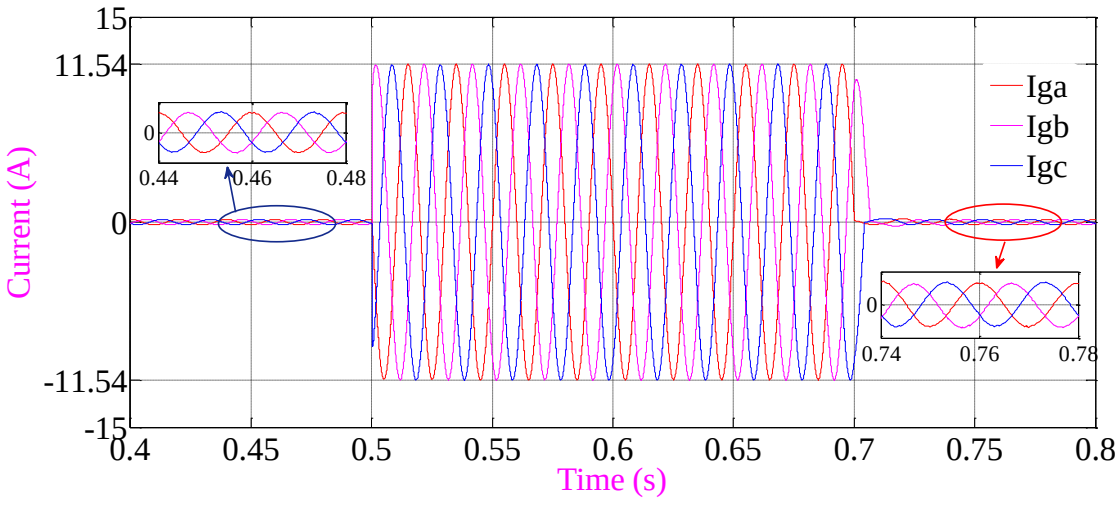

(a)

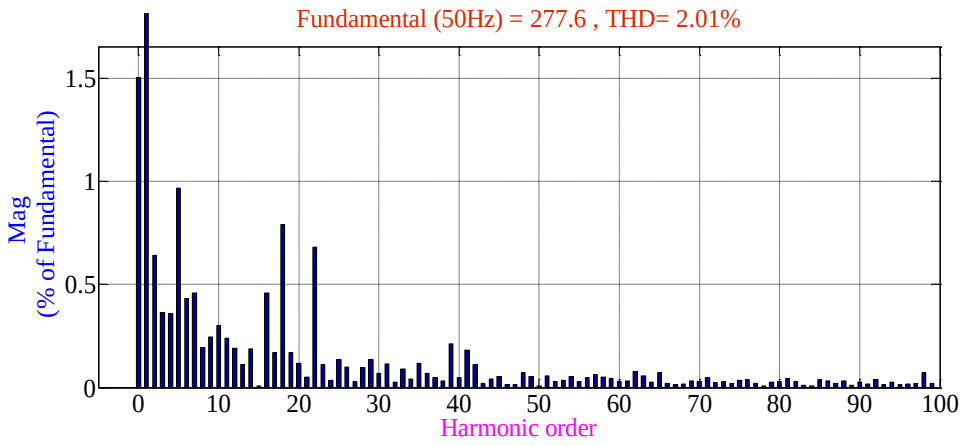

(b)

Figure 9: (a) The output current waveforms of a three-phase system with an LCL filter. (b) Fast Fourier Transform (FFT) analysis of the photovoltaic (PV) inverter system with an LCL filter.

Figure 9 displays the current waveforms and Fast Fourier Transform (FFT) analysis of the current in the inverter system equipped with an LCL filter.

IV. CONCLUSION

This paper presents a simple, accurate, and methodical approach to designing an LCL filter, which serves as an intermediary between a three-phase power converter and the utility grid. The purpose of this filter is to mitigate the harmonics in the current waveform generated by the power converter's switching frequency. The proposed design methodology exhibits characteristics of simplicity, efficiency, and a specific focus on meeting the grid code requirements. In contrast to traditional design methodologies, the proposed method exhibits a higher degree of simplicity and directness. Additionally, the design considers four essential criteria: adherence to reactive volt-ampere (VAR) limits, optimal filter volume, total harmonic distortion (THD) ≤ 0.003, and appropriate resonance frequency selection. The filter parameters obtained were evaluated using the MATLAB-Simulink software tool. The simulation results demonstrate that the proposed design methodology exhibits high reliability, efficiency, and effective filtering capabilities. The simulation results demonstrate that utilising this design methodology effectively reduces over 98% of the current harmonics observed at the output of the converter.

REFERENCES

[1] F.M.Gonzalez-Longatt, “Model of Photovoltaic Module in MATLAB” in Proc. 2do CongresoIberoamericano de Estudiantesde IngenieriaElectrica, Electronica y Computacion (II CIBELEC), 2005.pp.1-5.

[2] M.N.Kabir, Y.Mishra, G.Ledwich, Z.Y.Dong, and K.P.Wong, “Coordinated control of grid-connected photovoltaic reactive power and ……battery storage systems to improve the voltage profile of a residential distribution feeder,”IEEE Trans. Ind. Informat., vol. 10, no.2, pp. 967- ……977, May 2014.

[3] M. A. G. de Brito, L. Galotto, L. P. Sampaio, G. de Azevedo e Melo, and C. A. Canesin, "Evaluation of the main MPPT t echniques for …..photovoltaic applications," IEEE. Trans. Ind. Electron. vol. 60, no. 3, pp. 1156-1167, Mar. 2013.

[4] S.Gab-Su, S. Jong-Won, C. Bo-Hyung, and L. Kyu-Chan, "Digitally controlled current sensorless photovoltaic micro-converter for DC …..distribution," IEEE. Trans. Ind. Informat.,vol. 10, no. 1, pp. 117-126, Dec. 2014.

[5] C. Liang-Rui, T. Chih-Hui, L. Yuan-Li. And L.Yen-Shin, "A biological swarm chasing algorithm for tracking the PV maximum power …...point." IEEE Trans. Energy Convers., vol. 25, no. 2, pp. 484-493, May 2010.

[6] L. Yi-Hwa. H. Shyh-Ching, H.Jia-Wei, and L.Wen-Cheng, "A particle swarm optimization-based maximum power point tracng algorithm for …..PV systems operating under partially shaded conditions," IEEE Trans. Energy Convers., vol. 27, no. 4, pp. 1027-1035, Nov. 2012.

[7] T. K. Soon and S. Mekhilef, "Modified incremental conductance algorithm for photovoltaic system under partial shading conditions and load …..variations," IEEE Trans. Ind. Electron, vol. 61, no. 10, pp. 5384-5392, May 2014.

[8] X. Weidong and W. G. Dunford, "A modified adaptive hill climbing MPPT method for photovoltaic power systems,"in Proc. IEEE ……35thAnnu.Power Electron. Spec. Conf., 2004, vol. 3, pp. 1957-1963.

[9] N. Femia, G. Petrone, G. Spagnuolo, and M. Vitelli, "Optimization of perturb and observe maximum power point tracking method," IEEE …..Trans. Power Electron., vol. 20, no. 4, pp. 963-973, Jul. 2005.

[10] A. K. Abdelsalam, A. M. Massoud, S. Ahmed, and P. N. Enjeti, "High performance adaptive perturb and observe MPPT technique for ……photovoltaic-based microgrids," IEEE Trans. Power Electron., vol. 26, no. 4, pp. 1010-1021, Jun. 2011.

[11] A. Safari and S. Mekhilef, "Simulation and hardware implementation of incremental conductance MPPT with direct control method using ……CUK converter,"IEEE Trans. Ind. Electron., vol. 58, no. 4, pp. 1154-1161, Mar. 2011.

[12] X. Weidong, W. G. Dunford, P. R. Palmer, and A. Capel, " Application of centered differentiation and steepest descent to maximum power ……point tracking," IEEE Trans. Ind. Electron., vol. 54, no. 5, pp. 2539-2549, Aug. 2007.

[13] TeyKok Soon and Saad Mekhilef, "A fast- converging MPPT technique for photovoltaic system under fast - varying solar irradiation and …….load resistance," IEEE Trans. Ind. Informatics., vol. 11, no. 1, Feb. 2015.

[14] L. Fangrui, D. Shanxu, L. Fei, L. Bangyin, and K. Yong, " A variable step size INC MPPT method for PV systems," IEEE Trans. Ind. ……Electron., vol. 55, no. 7, pp. 2622-2628, Jun. 2008.

[15] S. Patel and W. Shireen, "Fast converging digital MPPT control for photovoltaic (PV) applications," in Proc. Power Energy Soc. Gen. ……Meeting, 2011, pp. 1-6.

[16] L. Kui-Jun and K. Rae- Young, "An adaptive maximum power point tracking based on a variable scaling factor for photovoltaic systems," ……IEEE Trans. Energy Convers., vol. 27, no. 4, pp. 1002-1008Nov. 2012.

[17] K. Tattiwong and C. Bunlaksananusorn, "Analysis design and experimental verification of a quadratic boost converter," IEEE Trans. Ind. ……Electron., vol. 54, no. 5, pp. 4075-4080, Aug. 2014.

[18] O. Lopez-Santos, L. Martinez-Salamero, G. Garcia, H. Valderrama-Blavi, D. Mercury, "Efficiency analysis of a Sliding Mode Controlled ……Quadratic Boost Converter," IET Power Electron., 2013, vol. 6, Iss 2, pp. 364-373.

